Scaling relations at the critical line and the period-doubling route for the sine map and the driven damped pendulum

P. Alstrøm,* B. Christiansen, P. Hyldgaard, M. T. Levinsen, and R. Rasmussen
Physics Laboratory I, H. C. Ørsted Institute, Universitetsparken 5, DK-2100 Copenhagen Ø, Denmark
(Received 18 February 1986)

With basis in number theory, scaling relations for the sine map have been investigated, generalizing the work of Shenker which concentrated on "golden" rotation numbers (equivalents of the golden mean). Scaling functions are found, and exponents associated with the convergence rate, defined for periodic irrationals. In the light of the fact that the step structure obtained by iterations of the sine map exhibits a kind of self-similarity, correspondences to scaling laws for Cantor's discontinuum have been studied. We define a "similarity dimension" which is found to scale with Shenker's exponents, as the sine map attains a zero-slope third-order inflection point. Moreover, we examine the subset of steps having associated a denominator, which is a power of 2, and find a correlated fractal dimension which is half the fractal dimension of the original Cantor set. Inspired by these results, we have considered the driven damped pendulum equation and tried to recover corresponding scaling laws. Surprisingly, another scaling exponent $\tilde{z}\cong 1.5$ is found where Shenker's exponent $z\cong 1.05$ was to be expected. Finally, the period-doubling route to chaos inside the hysteretic region for the pendulum equation is discussed, and qualitative agreement with the behavior of the one-dimensional sine map obtained.

INTRODUCTION

In the last years scaling properties have been investigated extensively, both for structures obtained by iterating real maps[1-8] and for structures found at certain critical lines in the parameter space for differential equations involving two competing frequencies.[6,8-11]. It has been confirmed[10] that the fractal found along such critical lines, recognized as sets of points where hysteresis sets in,[6,10] has associated the same fractal dimension and decay exponents as those found for the complete devil's staircase achieved by iterating a circle map with a zero-slope third-order inflection point.[3,6] However, not only the scaling properties associated with such maps but also the features when such a map is approached have been investigated and universal scaling parameters found.[3,6]

In this paper, this investigation is continued. The scaling parameters found are put into a number-theoretical description and correlations discussed. We also consider relations to the self-similar fractal called Cantor's discontinuum[12,13] with the purpose of studying the properties inherited from the self-similar step structure.

We close the paper by examining the transition to chaos through period doubling, and present analog computations of the cascades in the driven damped pendulum equation. We discuss similarities with the structure provided by the sine map, although the Poincaré map for the pendulum equation in known not to be one-dimensional in this regime.[6]

APPROACHING THE CRITICAL LINE

In his investigation of scaling relations at the irrational number $R_{\rm gm}=(\sqrt{5}-1)/2$, Shenker[3] considered the behavior of three quantities. To introduce these, one uses the representation of real numbers in continued fractions:

$$[a_1,a_2,a_3,\dots]=\cfrac{1}{a_1+\cfrac{1}{a_2+\cfrac{1}{a_3+\cdots}}}\ , \tag{1}$$

with a_n positive integers.

It is well-known that every rational P/Q (between 0 and 1) can be written as a finite continued fraction in a unique way as

$$\frac{P}{Q}=[a_1,\dots,a_n],\ \ a_1,a_2,\dots,a_{n-1}\geqq 1,\ a_n\geqq 2\ , \tag{2}$$

and every irrational can be written uniquely as an infinite continued fraction, e.g., $R_{\rm gm}=[1,1,1,\dots]$. For every irrational $R=[a_1,\dots,a_n,\dots]$, the sequence of rationals

$$R_n=\frac{P_n}{Q_n}=[a_1,a_2,\dots,a_n],\ \ n=1,2,3,\dots \tag{3}$$

converges towards R.

If $g(x)$ is some smooth orientation-preserving circle map $[g(x+1)=g(x)+1]$, the "translated" map

$$f_\mu(x)=\mu+g(x) \tag{4}$$

is too. If, moreover, μ is such that a sequence of Q_n numbers $x_0,x_1,\dots,x_{Q_n-1}$ exists with

$$x_i=f_\mu(x_{i-1})\ \text{ for } i=1,2,\dots,Q_n-1\ , \tag{5a}$$

and

$$x_0=f_\mu(x_{Q_n-1})-P_n\ , \tag{5b}$$

the rotation number

$$R_g(\mu)=\lim_{n\to\infty}\frac{f_\mu^n(x_0)-x_0}{n} \tag{6}$$

equals R_n. In this case $\{x_0,\ldots,x_{Q_n-1}\}$ is called an R_n-cycle, which furthermore is said to be stable if

$$D_\mu=\frac{df_\mu^{Q_n}}{dx}(x_i)=\prod_{i=0}^{Q_n-1}\frac{dg}{dx}(x_i) \tag{7}$$

is less than 1. Generally,[14] for every μ with $R_g(\mu)=R_n$ there is a unique stable R_n-cycle, and among such μ's, one can be found (call it μ_n) where D_μ is minimal. This μ_n is denoted as the superstable point on the R_n step, which is an interval $\Delta\mu_n$ of μ's where $R_g(\mu)=R_n$. For simplicity, we set $D_n=D_{\mu_n}$.

If x_0 is chosen as the point in the stable R_n-cycle having the smallest derivative dg/dx, a distance d_n can be defined as

$$d_n=f_{\mu_n}^{Q_n-1}(x_0)-(x_0+P_{n-1})\ . \tag{8}$$

As n tends to infinity, d_n will approach zero.

The three quantities investigated by Shenker are $\mu_{n+1}-\mu_n$, d_n, and D_n. For every set of circle maps $g_\varepsilon\to g$, where the subscript ε indicates the minimal derivative, i.e.

$$\varepsilon=\min_x\left\{\frac{dg_\varepsilon}{dx}(x)\right\}\to\min\left\{\frac{dg}{dx}(x)\right\}\ , \tag{9}$$

we get sequences $\mu_{n+1}(\varepsilon)-\mu_n(\varepsilon)$, $d_n(\varepsilon)$, and $D_n(\varepsilon)$ converging towards $\mu_{n+1}-\mu_n$, d_n, and D_n. If $\varepsilon\to 0$, i.e., g has a vanishing derivative in some point x_0 and thus a zero-slope inflection point, this point will appear in some R_n-cycle at every superstable point μ_n, and $D_n(0)=0$. The line $\varepsilon=0$ in (μ,ε) space is called the critical line.

Regarding the case where g has a third-order inflection point x_0, Shenker finds for the Fibonacci sequence $R_n\to R_{\rm gm}$ universal exponents $y_{\rm gm}$ and $x_{\rm gm}$, such that

$$\mu_{n+1}(\varepsilon)-\mu_n(\varepsilon)\sim Q_n^{-y_{\rm gm}}\ , \tag{10a}$$

where

$$y_{\rm gm}=\begin{cases}2 & \text{for } \varepsilon>0\\ 2.1644\ldots & \text{for } \varepsilon=0\ ,\end{cases} \tag{10b}$$

while

$$d_n(\varepsilon)\sim Q_n^{-x_{\rm gm}}\ , \tag{11a}$$

where

$$x_{\rm gm}=\begin{cases}1 & \text{for } \varepsilon>0\\ 0.5268\ldots & \text{for } \varepsilon=0\ .\end{cases} \tag{11b}$$

The case $\varepsilon>0$ can be solved analytically. Shenker also considers the behavior as $\varepsilon\to 0$ and finds that all of the above three quantities depend only on the product $\varepsilon Q_n^{z_{\rm gm}}$, with universal scaling parameter $z_{\rm gm}=1.0537\ldots$. As indicated by Feigenbaum *et al.*,[4] it is possible to show that $z_{\rm gm}=2x_{\rm gm}$, and generally

$$z_{\rm gm}(n)=(n-1)x_{\rm gm}(n) \tag{12}$$

if g has order n.

Finally, Shenker concludes that y and x (or z) are unchanged for every irrational of the form $[a_1,\ldots,a_n,1,1,1,\ldots]$, while the irrationals $[n,n,n,\ldots]$ with $n>1$ have different values of y and x (the values y and x are found to be well-defined in the same way as $y_{\rm gm}$ and $x_{\rm gm}$). To this end, we mention that every two irrationals ξ and η having the same form from a given step, i.e., $\xi=[a_1,\ldots,a_n,c_1,c_2,\ldots]$ and $\eta=[b_1,\ldots,b_n,c_1,c_2,\ldots]$, are equivalent, i.e., some integers a,b,c,d exist such that[5,15]

$$\xi=\frac{a\eta+b}{c\eta+d},\quad ad-bc=\pm 1\ , \tag{13}$$

e.g., the irrationals $[a_1,\ldots,a_n,1,1,1,\ldots]$ are equivalent to $R_{\rm gm}$. Further, every periodic irrational

$$R=[a_1,a_2,a_3,\ldots],\quad a_{n+k}=a_n \text{ for } n\geqq n_0 \tag{14}$$

(k is called the period) is a root of an irreducible quadratic equation with integral coefficients, and using the fact that[15]

$$\frac{Q_{n-1}}{Q_n}=[a_n,a_{n-1},\ldots,a_2,a_1]\ , \tag{15}$$

periodic irrationals with period k can be ascribed to a convergence rate

$$l=\lim_{n\to\infty}\left[\frac{Q_n}{Q_{n+k}}\right]^{1/k}\ . \tag{16}$$

In particular, for 1-periodic irrationals $R=[n,n,n,\ldots]$ like $R_{\rm gm}$, $l=R$. Moreover, l is evidently the same for equivalent periodic irrationals.

It therefore appears natural to study the scaling parameters as a function of the convergence rate, and hence we start seeking whether scaling laws

$$\mu_{n+1+mk}(\varepsilon)-\mu_{n+mk}(\varepsilon)\sim Q_{n+mk}^{-y} \tag{17}$$

and

$$d_{n+mk}(\varepsilon)\sim Q_{n+mk}^{-x} \tag{18}$$

exist, and if so, whether y and x are invariant under the equivalence (13). Again, the case $\varepsilon>0$ can be solved analytically using Denjoy's theorem,[16] which leads to the earlier given values $y=2$ and $x=1$. For $\varepsilon=0$, things are quite different. Indeed, universal scaling relations (17) and (18) are found. For the sine map

$$f_\mu(x)=\mu+x-\frac{1}{2\pi}\sin(2\pi x)\ , \tag{19}$$

some results are listed in Table I.

For the sake of clarity, equivalent numbers are represented in the table by one number only, but the invariance of x and y has been checked, e.g., for the 2-periodic numbers $[a,b,a,b,\ldots]$, the number $[b,a,b,a,\ldots]$ is found to have associated exactly the same values of x and y. Note that although the numbers $[1,2,3,1,2,3,\ldots]$ and $[3,2,1,3,2,1,\ldots]$ have the same convergence rate, they are not equivalent. Nonetheless, their associated values of x and y are still equal. This cir-

TABLE I. Convergence rate and the decay exponents x and y for some periodic irrationals.

R	l	x	y
[1,1,1,...]	0.618	0.527	2.164
[2,2,2,...]	0.414	0.524	2.175
[3,3,3,...]	0.303	0.517	2.195
[4,4,4,...]	0.236	0.511	2.220
[5,5,5,...]	0.193	0.496	2.244
[1,2,1,2,...]	0.518	0.516	2.180
[1,3,1,3,...]	0.457	0.498	2.204
[1,4,1,4,...]	0.414	0.483	2.227
[3,5,3,5,...]	0.243	0.502	2.225
[1,2,3,1,2,3,...]	0.436	0.516	2.192
[3,2,1,3,2,1,...]	0.436	0.516	2.192
[2,2,3,2,2,3,...]	0.374	0.523	2.188
[3,4,3,4,...]	0.268	0.514	2.208
[2,6,2,6,...]	0.268	0.486	2.240
[1,12,1,12,...]	0.268	0.392	2.356

cumstance is, however, not general. As examples, the irrationals [2,2,2,...] and [1,4,1,4,...], as well as [2,4,2,4,...] and [1,8,1,8,...], have the same convergence rate, but not the same scaling exponents. An interesting observation here is that the values of x and y follow more closely the values of the highest number in the periodic sequences as exemplified in the irrationals [3,4,3,4...], [2,6,2,6,...], and [1,12,1,12,...]. Anyhow, periodic irrationals with equal convergence rates can be characterized by a common scaling equation; for proof see the Appendix.

Moreover, we find the often tacitly assumed proportionalities

$$\Delta\mu_j \sim \mu_{j+1} - \mu_j \ , \tag{20}$$

$$\tilde{d}_j = \min_{i=1,2,\ldots,Q_j-1} \{x_i - x_0 - \lfloor x_i - x_0 + 0.5 \rfloor\} \sim d_j \tag{21}$$

($\lfloor\ \rfloor$ denotes the integer part) to be valid, $\tilde{d}_j$ is simply the shortest distance mod 1 from any x_i, $i \neq 0$, to x_0 [for the sine map (19), $x_0 = 0$]. As an example, in Fig. 1 we show $\ln\tilde{d}_j$ versus $\ln Q_j$ for the 2-periodic sequence converging towards $[3,1,3,1,\ldots] = (\sqrt{21}-3)/6$. It can be seen that the points fall on two parallel lines. In general, the points fall on n parallel lines for an n-periodic sequence.

Inspired by the work of Shenker, we have also considered the behavior as ε tends to zero , examining the sequence of sine maps $f_{\mu,\varepsilon}$ given by

$$f_{\mu,\varepsilon}(x) = f_\mu(x) + \frac{\varepsilon}{2\pi}\sin(2\pi x) \ . \tag{22}$$

We generally find scaling relations of the form

$$\Delta\mu_j(\varepsilon) = \Delta\mu_j(0)\sigma_\Delta(\varepsilon Q_j^z) \tag{23}$$

and

$$\tilde{d}_j(\varepsilon) = \tilde{d}_j(0)\sigma_d(\varepsilon Q_j^z) \ , \tag{24}$$

with $z = 2x$. Additionally, σ_Δ is found to be an exponential function, i.e.,

$$\sigma_\Delta(t) = a^{-t} \tag{25}$$

($a > 1$ nonuniversal, with $\ln a$ of order 1), when $t \lesssim 1$. Figure 2(a) shows $\Delta\mu_j(\varepsilon)$ for the Fibonacci sequence in a semilogarithmic plot. By plotting the slopes obtained in a double-logarithmic plot, Fig. 2(b), Shenker's scaling parameter z_{gm} is recovered.

Concerning the distance $\tilde{d}_j$, we find as expected that $\sigma_d(t)$ at $t = 0$ is linear in the argument,

$$\sigma_d(t) = 1 - bt \tag{26}$$

(in contrast to $\ln a$, $b \ll 1$). Figure 3(a) shows the Fibonacci sequence case, and the slopes determined as $\varepsilon \to 0$ again give the value of z to be z_{gm}. Moreover, knowing that[3] $\tilde{d}_j(\varepsilon) \sim Q_j^{-1}$ for fixed and sufficiently large Q_j, we conclude that

$$\tilde{d}_j(\varepsilon) \sim Q_j^{-1}\varepsilon^{-(1-x)/z} \tag{27}$$

in this limit. Figure 3(b) shows $\ln\tilde{d}_j(\varepsilon)$ versus $\ln\varepsilon$, and indeed we find this "limit" slope in accordance with the one calculated from Shenker's value of x, i.e., $(1-x)/2x = 0.4490\ldots$.

In the same fashion, several other periodic sequences have been investigated. In all cases we find the relation $2x = z$ fulfilled. Also, for an n-periodic sequence, we find n parallel lines in the plots analogous to Figs. 2(b) and 3(b).

In a recent work by Jensen *et al.*,[6] the averaged values of $\Delta\mu$ and $\tilde{d}$,

$$\langle\Delta\mu\rangle(Q) = \langle\Delta\mu(P/Q)\rangle_P \ , \tag{28}$$

$$\langle\tilde{d}\rangle(Q) = \langle\tilde{d}(P/Q)\rangle_P \ , \tag{29}$$

respectively, were also considered, and they find that

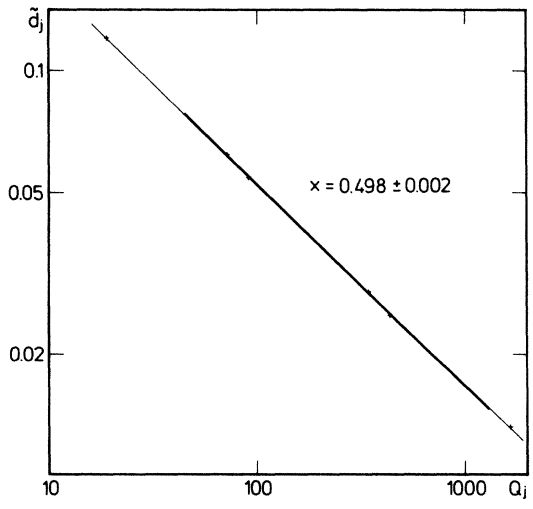

FIG. 1. Distances $\tilde{d}_j$ vs Q_j in a double-logarithmic plot for the [3,1,3,1,...] sequence. Note the two parallel lines. The slope gives the value of the scaling exponent x.

$$\langle \Delta\mu \rangle(Q) \sim Q^{-\bar{y}} , \tag{30}$$

while

$$\langle \tilde{d} \rangle(Q) \sim Q^{-\bar{x}} , \tag{31}$$

with $\bar{y} \cong 2.29$ and $\bar{x} \cong 0.43$. Writing

$$\bar{y} = 2/\bar{D} , \tag{32}$$

$\bar{D}$ equals, within the uncertainty, the fractal dimension $D=0.87$. In this connection, we have investigated the behavior of these scaling parameters when ε is positive, but tends to zero. Using the same procedure as above, cf. Figs. 4 and 5, we obtain similar proportionalities,

$$\langle \Delta\mu \rangle(Q,\varepsilon) = \langle \Delta\mu \rangle(Q,0)\bar{\sigma}_{\Delta}(\varepsilon Q^{\bar{z}}) \tag{33}$$

and

$$\langle \tilde{d} \rangle(Q,\varepsilon) = \langle \tilde{d} \rangle(Q,0)\bar{\sigma}_{d}(\varepsilon Q^{\bar{z}}) , \tag{34}$$

with

$$\bar{\sigma}_{\Delta}(t) = \bar{a}^{-t} , \tag{35}$$

$$\bar{\sigma}_{d}(t) = 1 - \bar{b}t \tag{36}$$

($t \lesssim 1$), and $\bar{z} \cong 0.88$, which is identical to $2\bar{x}$ within the uncertainty. However, a limit behavior like (27) is not attained in the (Q,ε) region where it is possible to find $\langle \tilde{d} \rangle$.

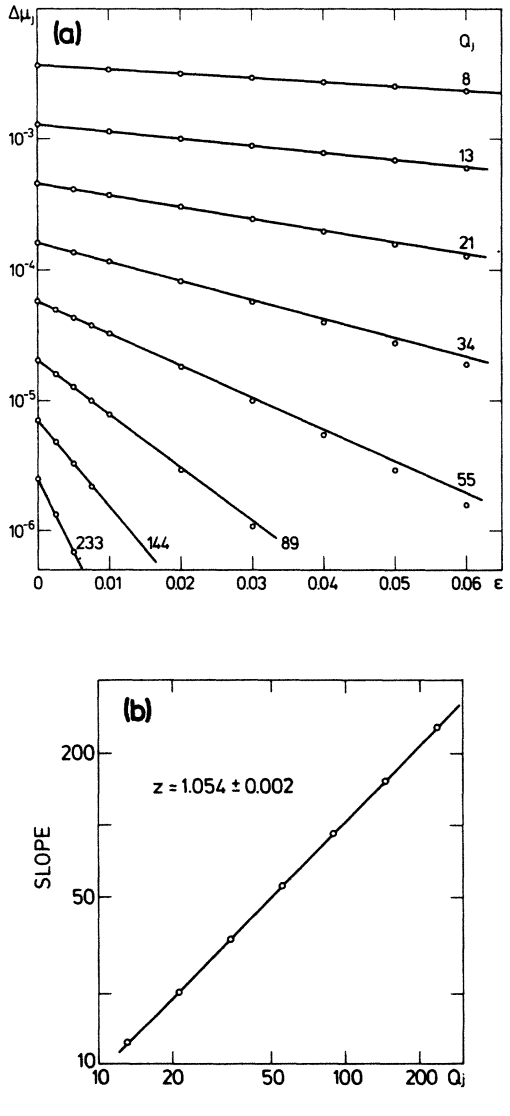

FIG. 2. (a) Step size $\Delta\mu_j$ vs ε in a semilogarithmic plot for the Fibonacci sequence. (b) The slopes are plotted vs Q_j on double-logarithmic paper in order to find the scaling exponent z. The unit on the ordinate axis is chosen such that tha intersection point at $Q_j = 1$ is $\ln a$, cf. Eq. (25).

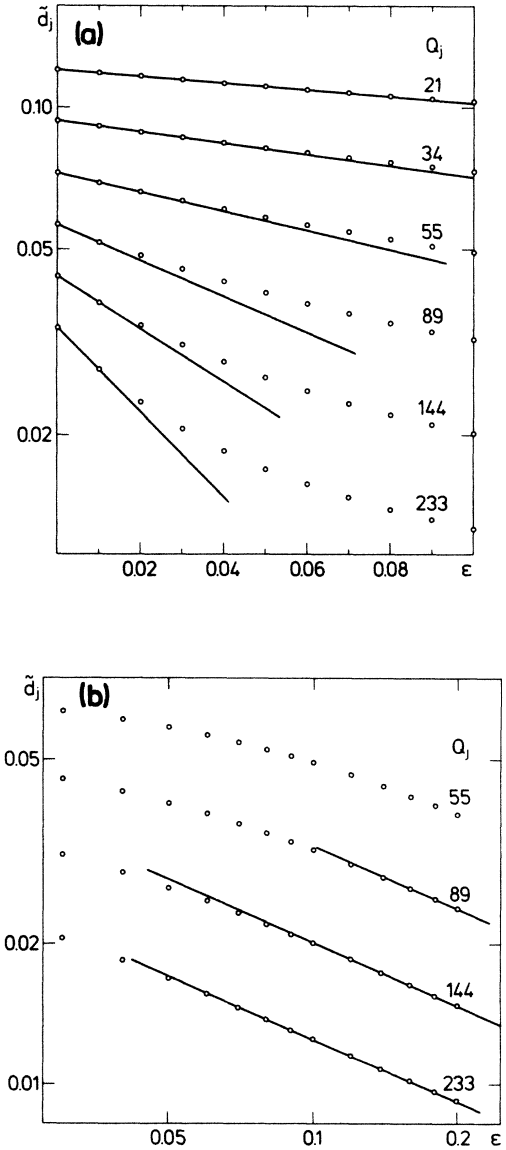

FIG. 3. (a) Distance $\tilde{d}_j$ vs ε in a semilogarithmic plot for the Fibonacci sequence. (b) By plotting $\ln\tilde{d}_j$ vs $\ln\varepsilon$, z (or x) can also be found from the behavior of $\tilde{d}_j(\varepsilon)$ at large values of εQ_j. The slopes are all 0.449 ± 0.001.

We remark that our value of $\bar{z}$ is different from the unit value proposed by Jensen *et al.* However, if we calculate the measure M of quasiperiodic orbits, we find, introducing the Euler function $\phi(Q)$ as the number of irreducible fractions P/Q with denominator Q ($0 \leq P < Q$), that

$$M(\varepsilon) \sim \sum_{\substack{Q \\ \varepsilon Q^{\bar{z}} > 1}} \phi(Q) \langle \Delta\mu \rangle(Q) \sim \sum_{\substack{Q \\ Q > \varepsilon^{-1/\bar{z}}}} Q Q^{-\bar{y}} \sim \varepsilon^{\bar{\beta}} , \tag{37}$$

where

$$\bar{\beta} = (\bar{y} - 2)/\bar{z} \cong 0.33 , \tag{38}$$

in excellent agreement with the value of β obtained in a more rigoristic way from the equality

$$D = 1 - \frac{\beta}{\nu} , \tag{39}$$

where ν is the exponent belonging to the "correlation length" ξ,

$$\xi \sim \varepsilon^{-\nu} , \tag{40}$$

indicating the scale $r_0 = 1/\xi$, where a crossover from the fractal to the continuous nature appears.

Examining the behavior of the number $N(r,\varepsilon)$ of steps $\Delta\mu(\varepsilon)$ larger than the scale r, Jensen *et al.* obtain $\nu \cong 2.63$. A proper correlation length $\bar{\xi}$ is here determined by the condition that

$$\varepsilon Q^{\bar{z}} \sim \sigma(\bar{\xi} \langle \Delta\mu \rangle(Q)) \tag{41}$$

for some scaling function σ. Using the behavior (30), we find

$$\bar{\xi} \sim \varepsilon^{-\bar{\nu}}, \quad \bar{\nu} = \bar{y}/\bar{z} , \tag{42}$$

with $\bar{\nu} \cong \nu$, and by (32) and (38) we end up with the relation

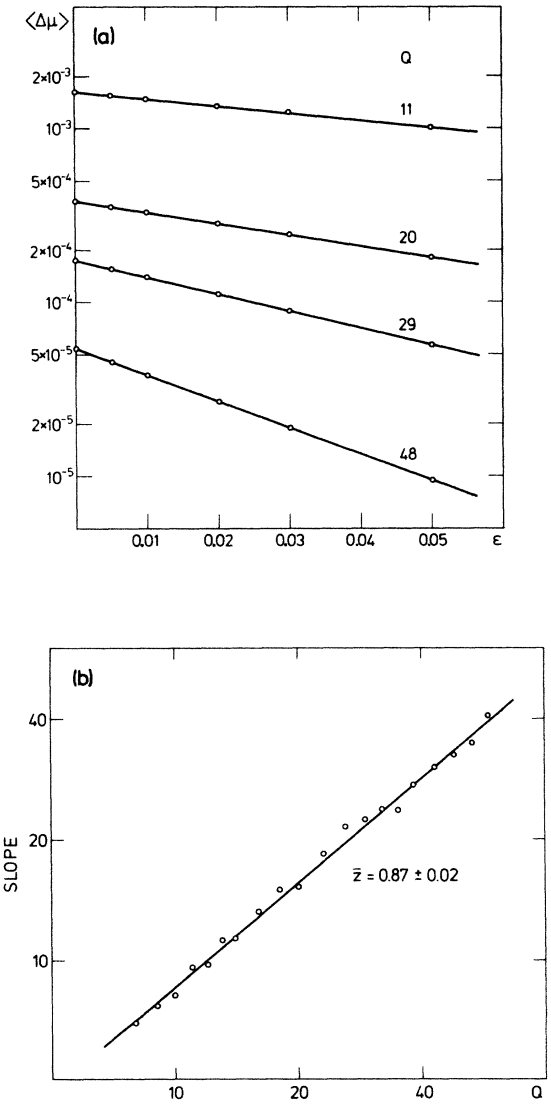

FIG. 4. (a) Mean step size $\langle \Delta\mu \rangle(Q)$ vs ε in a semilogarithmic plot for some values of Q. (b) The slopes are plotted vs Q on double-logarithmic paper in order to find the scaling exponent $\bar{z}$. The unit on the ordinate axis is chosen such that the intersection point at $Q = 1$ is $\ln\bar{a}$, cf. Eq. (35).

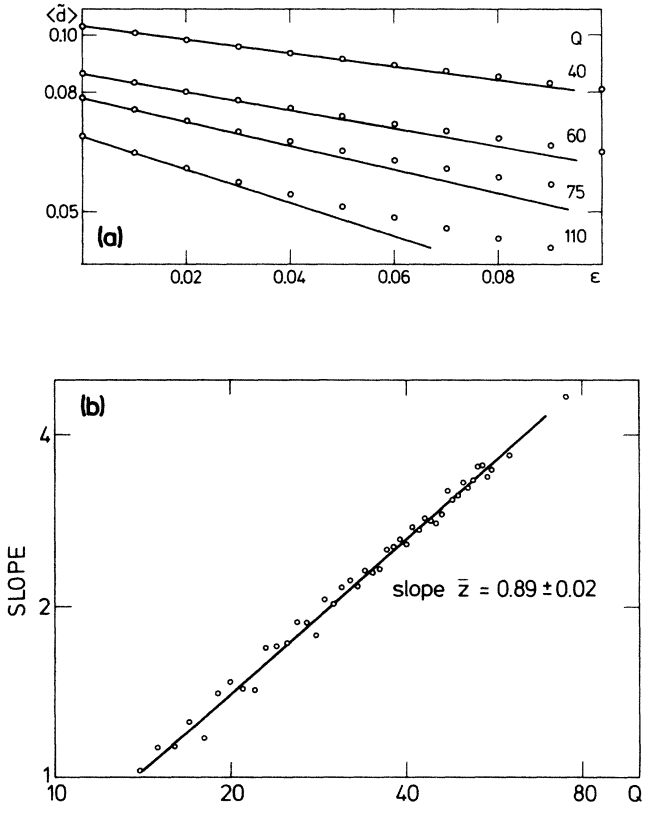

FIG. 5. (a) Mean distance $\langle \tilde{d} \rangle(Q)$ vs ε in a semilogarithmic plot for some values of Q. (b) The slopes obtained as $\varepsilon \to 0$ are plotted vs Q on double-logarithmic paper in order to find the scaling exponent $\bar{z}$. The unit on the ordinate axis is chosen such that the intersection point at $Q = 1$ is $\bar{b}$, cf. Eq. (36).

$$\bar{D}=1-\frac{\bar{\beta}}{\bar{\nu}} \tag{43}$$

for the scaling exponents belonging to the mean values, which is completely analogous to (39).

SIMILARITIES WITH CANTOR'S DISCONTINUUM

Due to the nice kind of self-similarity observed in the step structure of $R_g(\mu)$ [g given by (19)], see Fig. 6, we have been encouraged to investigate the connections between the Cantor set $\{\mu \mid R_g(\mu)$ is irrational$\}$ and Cantor's discontinuum C obtained by successively removing the middle thirds of remaining intervals starting with the unit interval (Fig. 7). One simple relation valid for strictly self-similar Cantor sets like C is that

$$N_j r_j^{D_s}=1 , \tag{44}$$

where $N_j=N_1^j$ ($r_j=r_1^j$) is the number (length) of the remaining intervals at level j in the creation of the Cantor set. D_s is called the similarity dimension[13] and is independent of the level j. Moreover, Hausdorff has shown that $D_s=D$.[17]

For Cantor's discontinuum and similar sets, the "holes" correspond to the steps $\Delta\mu$ for the circle map. At any level j, the distances $s_{j,m}$, $m=1,2,\ldots,N_j$, between the holes is $s_{j,m}=r_j$, and the condition (44) ensures that

$$s_{j,m}^D=\sum_{k=(m-1)N_{i-j}+1}^{mN_{i-j}} s_{i,k}^D, \quad j\leq i \tag{45}$$

particularly for $i=j+1$,

$$s_{j,m}^D=\sum_{k=(m-1)N_1+1}^{mN_1} s_{j+1,k}^D , \tag{46}$$

N_{i-j} is the number of distances between holes in the interval $s_{j,m}$. For the Cantor set C, $N_1=2$, and (46) simply reads

$$s_{j,m}^D=s_{j+1,2m-1}^D+s_{j+1,2m}^D . \tag{47}$$

Recently, (45)–(47) have been utilized to estimate the fractal dimension locally for the step structure obtained from the sine map (19).[18] For the case $R=R_{gm}$ it is known that $\Delta\mu(P_{j+1}/Q_{j+1})$ is the largest step between $\Delta\mu(P_{j-1}/Q_{j-1})$ and $\Delta\mu(P_j/Q_j)$, and a kind of "similarity dimension" $D_{s,j}$ can thus be found from an equation equivalent to (47),

$$s_{j,1}^{D_{s,j+1}}=s_{j+1,1}^{D_{s,j+1}}+s_{j+1,2}^{D_{s,j+1}} , \tag{48}$$

where $s_{j,m}$, $m=1,2$, denotes the μ distance between $\Delta\mu(P_j/Q_j)$ and $\Delta\mu(P_{j-m}/Q_{j-m})$. A calculation of $D_{s,j}$ from (48) gives, almost independently of j, $D_{s,j}=D_s=0.858$, which is almost equal, but definitely smaller than D.

Nevertheless, the behavior of $1-D_{s,j}$ is found to be characterized by the same scaling parameters as the quantities treated in the last section when the critical line is approached. This is illustrated by Figs. 8(a) and 8(c), show-

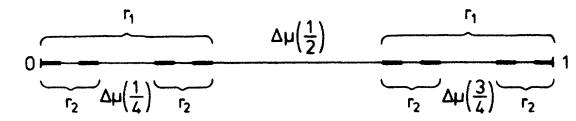

FIG. 7. Cantor's discontinuum can be created by successively removing $N_{n-1}=2^{n-1}$ intervals of length $\Delta\mu(P/2^2)=3^{-n}$.

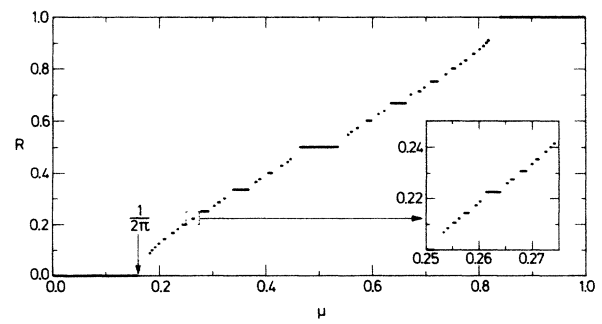

FIG. 6. Rotation number $R=R_g(\mu)$ for the sine map at $\varepsilon=0$. Note the self-similar nature of the staircase under magnification.

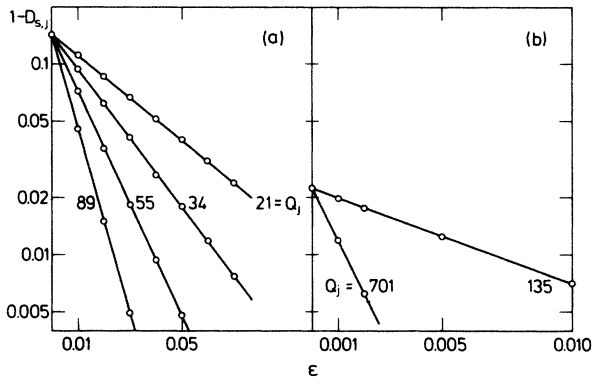

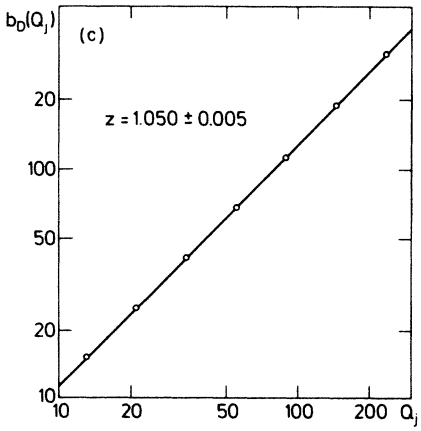

FIG. 8. Codimension $1-D_{s,j}$ vs ε in a semilogarithmic plot. (a) For the Fibonacci sequence. (b) For [5,5,5] and [5,5,5,5]. (c) Plotting the slopes vs Q_j on double-logarithmic paper, the scaling exponent z is recovered for the Fibonacci sequence.

ing that

$$1-D_{s,j}(\varepsilon)=(1-D_s)\exp[-\varepsilon b_D(Q_j)]\ , \tag{49a}$$

where

$$b_D(Q_j)\sim Q_j^z\ , \tag{49b}$$

and z is found to be the same as that obtained in the last section. To this end, we stress that the "small" value of $D-D_s$ by no means is responsible for the linear behavior of $\ln[1-D_{s,j}(\varepsilon)]$, e.g., for the sequence of rationals converging towards [5,5,5,...] where $D_{s,j}^{(0)}$ is found to be $D_{s,j}^{(0)}=D_s=0.978$, nice straight lines are still found, cf. Fig. 8(b), and the slopes change exactly according to the value of z obtained as $2x=0.992$ from Table I.

To achieve a complete devil's staircase for Cantor sets like C (Fig. 7), one imagines a homogeneous distribution of mass $m(x)$ on the Cantor set which adds up to a total mass 1. Then the increasing map

$$\phi(\mu)=\int_0^\mu m(x)dx \tag{50}$$

is a complete devil's staircase having all values between 0 and 1, and all μ on a step $\Delta\mu$ associated with a hole in the Cantor set will have a rational value of $\phi(\mu)$. If $\phi(\mu)=P/Q$ (irreducible), we write $\Delta\mu$ as $\Delta\mu(P/Q)$. It is readily shown that for $Q=N_n$

$$\Delta\mu(P/Q)=\langle\Delta\mu(P/Q)\rangle_P\sim Q^{-1/D}\ , \tag{51}$$

in sharp contrast to the behavior obtained from the sine map staircase $R_g(\mu)$ [cf. (30) and (32)].

The difference is due to the fact that while steps occur at every rational value of $R_g(\mu)$, steps only occur for values of $\phi(\mu)$ of the form P/N_n, P,n any integers, e.g., for Cantor's discontinuum, all steps are of the form $P/2^n$, P odd, and

$$\Delta\mu(P/2^n)=3^{-n}=(2^n)^{-1/D} \tag{52}$$

(see Fig. 9). Therefore, when counting the number $N(r)$ of steps larger than a given scale $r=\Delta\mu(P_0/Q_0)$, $Q_0=N_n$, we get

$$N(r)=\sum_{\substack{P/N_n\\ m<n}} 1=N_{n-1}-1\sim Q_0\ , \tag{53a}$$

while the counting if steps for all rationals are represented, and we assume r to be independent of P_0 (and decreasing with Q_0), gives

$$N(r)=\sum_{\substack{P/Q\\ Q<Q_0}} 1=\sum_{Q<Q_0}\phi(Q)$$
$$=\frac{3}{\pi^2}Q_0^2+O(Q_0\ln Q_0)\sim Q_0^2\ . \tag{53b}$$

Since

$$N(r)\sim r^{-D} \tag{54}$$

in both cases, a factor of 2 will occur in the step size decay exponent for the latter case (proposing $\bar{D}=D$) but not for the former.

Noticing this fact, it is a natural question to raise whether a fractal dimension D_2 equal to half the value of D will be found for the Cantor set obtained by successively removing intervals $\Delta\mu(P/N_n)$, calculated from iterating the sine map, from a total interval of length

$$L=\sum_{P/N_n}\Delta\mu(P/N_n)\ . \tag{55}$$

In Fig. 10, the most simple case $N_1=2$ is considered and $N(r)$ shown versus r in a double-logarithmic plot. Indeed, a slope $D_2\cong D/2$ is found, emphasizing the close connection to the scaling in Cantor's discontinuum.

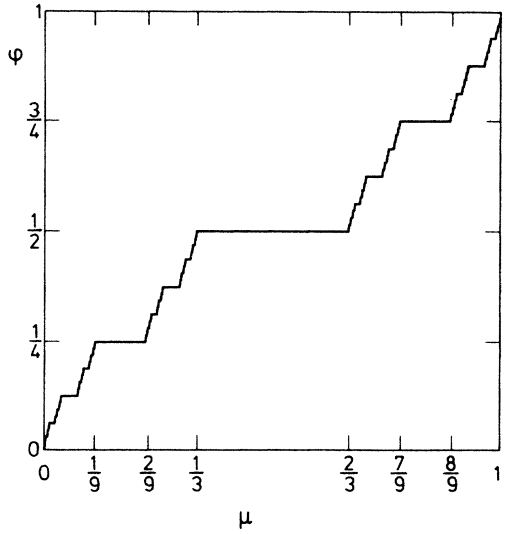

FIG. 9. Complete devil's staircase $\phi(\mu)$ obtained for Cantor's discontinuum.

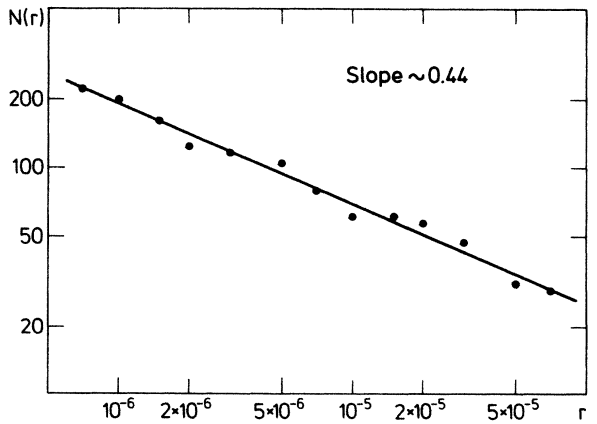

FIG. 10. Number of steps $N(r)$ larger than the scale r on double-logarithmic paper for the subset of step sizes in the sine map staircase $R_g(\mu)$ consisting of the step sizes of the form $\Delta\mu(P/2^n)$. The slope gives the related fractal dimension.

THE DRIVEN DAMPED PENDULUM

In earlier works,[10] we have considered the scaling properties (especially the fractal dimension) of the fractal obtained along the critical line for the driven damped pendulum system described by the normalized equation

$$\ddot{\phi}+G\dot{\phi}+U(\phi)=I+A\sin(\omega t)\,, \tag{56}$$

where ϕ is the phase, G is the damping constant, $U(\phi)$ is a periodic function, and the right-hand side of the equation is the external oscillating force. The rotation number R is the ratio between the two frequencies ω and $\langle\dot{\phi}\rangle=\lim_{T\to\infty}[\phi(T)/T]$,

$$R=\frac{\langle\dot{\phi}\rangle}{\omega}\,, \tag{57}$$

and on an I-R curve, the critical point is (if present) found where the hysteresis sets in. At every rational $R=P/Q$, a step is supposed to occur, and its size $\Delta I(P/Q)$ at the critical line has been used to estimate the fractal dimension by the counting method, cf. (54), as well as decay exponents for different converging sequences of rationals.

Here, the scaling properties when the critical line is approached have been considered. Typically, I-R curves obtained on an analog computer (EAI 680) look like those shown in Fig. 11, where $U(\phi)$ is chosen to be $\sin\phi$. Every curve is seen to be 'single-valued' for $I>I_0$ and hysteretic for $I<I_0$ for some critical value I_0 of I. For $R=P/Q$, the step size $\Delta I(P/Q)$ falls off when G is increased, and the step moves up in parameter I. It is therefore reasonable to believe that $I-I_0$ or $G-G_0$ can be used as the parameter ε, (I_0,G_0) being the critical point.

To this end, we are aware of the fact that ε can be more properly defined as the smallest value of the derivative of the Poincaré map which certainly is a circle map in the nonhysteretic regime, but crinkles up at the onset of hysteresis.[6] This definition of ε is, of course, only well-defined for irrational rotation numbers; for rational R, a width $\Delta\varepsilon(R)$ will exist but tend to zero as the denominator Q of R tends to infinite. However, the definition is not practical because of the large amount of computations needed. Furthermore, to achieve a sufficiently low scatter in the value of ε, a large amount of computer time will be required. Finally, generically it is to be expected that ε is proportional to $I-I_0$ and $G-G_0$ near the critical line.

Nonetheless, the results obtained are surprising. Considering the Fibonacci fractions P_j/Q_j, and assuming a behavior

$$\Delta I_j(I-I_0)=\Delta I_j(0)\exp[-(I-I_0)b_I(Q_j)] \tag{58a}$$

with

$$b_I(Q_j)\sim Q_j^{\tilde{z}}\,, \tag{58b}$$

Figs. 12(a) and 12(c) show that $\tilde{z}$ is found to be $\tilde{z}\cong 1.5$, substantially different from z. Here we have adopted $U(\phi)=\sin\phi+(\sin^3\phi)/6$ and $(A,\omega)=(1,1.76)$. Using $G-G_0$ instead, and claiming that

$$\Delta I_j(G-G_0)=\Delta I_j(0)\exp[-(G-G_0)b_G(Q_j)] \tag{59a}$$

with

$$b_G(Q_j)\sim Q_j^{\tilde{z}}\,, \tag{59b}$$

cf. Figs. 12(b) and 12(d), we reach the same result.

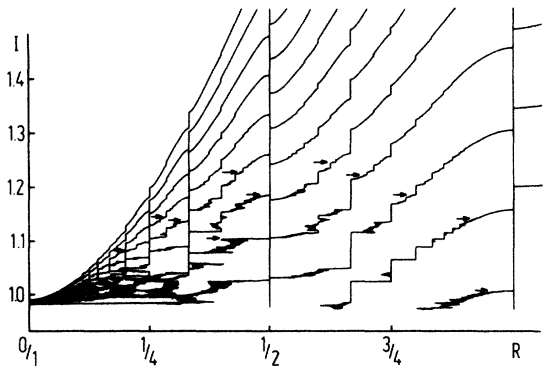

FIG. 11. I-R curves obtained for $U(\phi)=\sin\phi$, $A=1$, and $\omega=1.76$ by analog-computer calculations. The damping factor G is lowered successively by $\Delta G=0.08$, starting with $G=1.6$. Critical points are indicated by arrows.

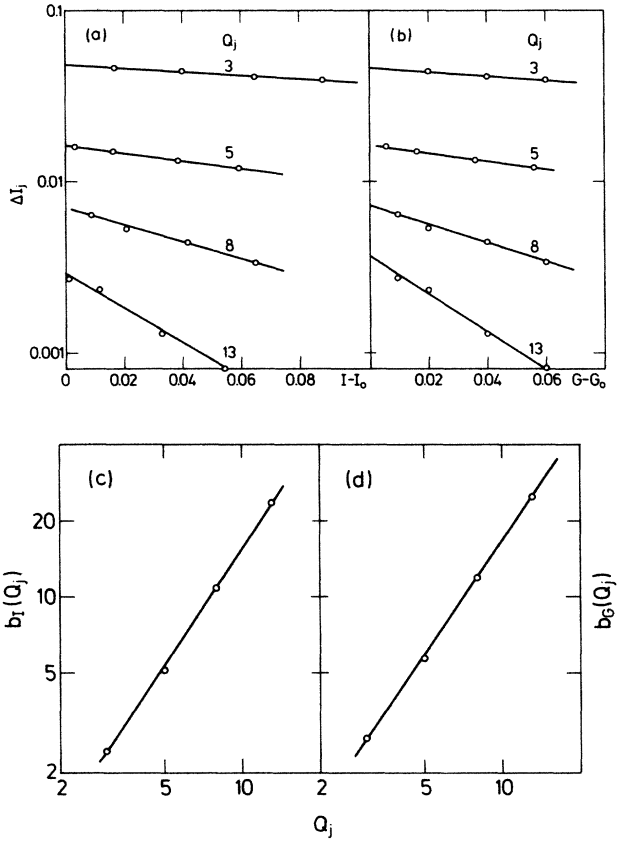

FIG. 12. Step size ΔI_j: (a) vs $I-I_0$, (b) vs $G-G_0$, in a semilogarithmic plot for the Fibonacci sequence. For the purpose here, the values of (I_0,G_0) have not been estimated in detail. By plotting the slopes of the least-squares lines (c) in (a) and (d) in (b) vs Q_j on double-logarithmic paper, a slope $\tilde{z}\simeq 1.5$ substantially larger than z is found.

Similar figures have been made for the [2,1,1,1,...] sequence, also giving $\tilde{z}$ at about 1.5. However, while the proportionality constant in (59b) is almost the same as that for the Fibonacci sequence, the proportionality constant in (58b) is found to be larger, emphasizing that $I-I_0$ only locally is proportional to ε, i.e.,

$$(I-I_0)(R)=c(R)\varepsilon\ , \tag{60}$$

with $c(R)$ continuous in the rotation number R. That $c(R)$ decreases when R decreases is expected, since the I-R curves (cf. Fig. 11) lie closer as R tends to zero.

We stress that the exponent $\tilde{z}$, within the uncertainty ($\sim 10\%$), is found to be unchanged if $U(\phi)$ is chosen to be $\sin\phi$, suggesting that $\tilde{z}$ is independent of the choice of $U(\phi)$. Moreover, from (58) and (59) it is seen that a change in the values of (I_0,G_0) only results in a parallel displacement of the lines in Figs. 12(a) and 12(b), and therefore leaves $\tilde{z}$ unchanged. A detailed knowledge of the critical line is therefore not necessary. However, since ε and $I-I_0$ are related through (60), and step sizes are measured in terms of ΔI, one might think that the result $\tilde{z}=1.5$ is an artifact of the procedure. To this end, we note that the value of I_0 is found almost constant at $R=[1,1,1,\ldots]$ [in both of the choices of $U(\phi)$ above]. Therefore, if G-R curves are used instead of I-R curves, step sizes $\Delta G_j(I-I_0)$ for a specific $I-I_0$ are obtained for every curve. Nevertheless, claiming that a scaling behavior (58) exists with ΔI_j interchanged by ΔG_j, we still get $\tilde{z}$ to be about 1.5. For the sake of completeness, we mention that also by considering $\Delta G_j(G-G_0)$ we are led to a value $\tilde{z}=1.5$.

Using the $G-R$ curves related to values of I near the almost-constant I_0 value for the Fibonacci fractions $[1,1,1]=\frac{2}{3},\ldots,[1,1,1,1,1,1,1]=\frac{8}{13}$, even the previously defined similarity dimension $D_{s,j}$ seems to give occasion for a behavior like that above. In Fig. 13, $\ln(1-D_{s,j})$ is plotted versus $I-I_0$ for $U(\phi)=\sin\phi$ and $(A,\omega)=(1,1.76)$. The change in the least-squares slopes is a factor of 2 and, in accordance with a value of $\tilde{z}$ about 1.5, indeed larger than z.

We suggest that this "discrepancy" with theory has its origin in the presence of noise, which smears out the step edges. This smearing is, in our analog computations, about $\delta I\sim 0.001$, or in other words about the same order as $\Delta I(\frac{8}{13}, I-I_0=0.05)$.

Here we should like to comment on the feasibility of measuring the similarity dimension for the Josephson equation. Since $D_{s,j}$ (for fixed G) is determined along a single curve, one would guess that large values of Q would yield the best result as the change in ε could then be minimized. However, from the result on the circle map [Fig. 8(a)] and from Fig. 13 for the Josephson equation, it is clear that large steps should be chosen to minimize the effect of the uncertainty in the precise position of the critical point. These two conflicting considerations raise severe doubt as to the value of this method.

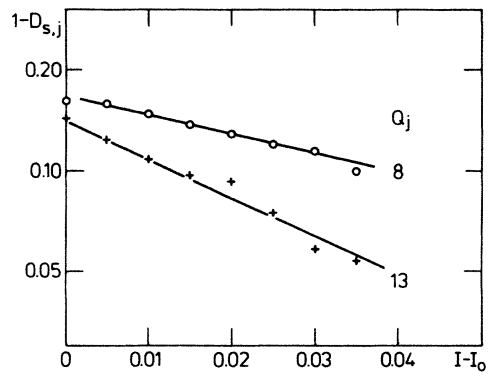

FIG. 13. Codimension $1-D_{s,j}$ vs $I-I_0$ in a semilogarithmic plot for the Fibonacci sequence.

THROUGH PERIOD DOUBLING TO CHAOS

Speculating on the similarities at the transition to hysteresis between the behavior on the steps for the driven damped pendulum and for circle maps, we have studied the features in the hysteretic region. When the steps move deeper inside the hysteretic region, bifurcations begin to affect the steps from the inside, and a period-doubling route to chaos is observed. In Fig. 14, such a situation is shown along the $\frac{1}{2}$ step; inside the hysteretic region, the Poincaré map is traced. However, the phase lock is still preserved, and is first lost well inside the chaotic regime.

The period-doubling route has here been examined by use of a low-frequency spectrum analyzer (HP3561A) to obtain spectra at different (negative) values of $I-I_0$. In Fig. 15, an example of how the spectra develop as the hysteretic region is entered is shown for $P/Q=\frac{3}{17}$. Figure 16 shows the associated I-R curves. It is noticed that even when the critical line is crossed, the noise back-

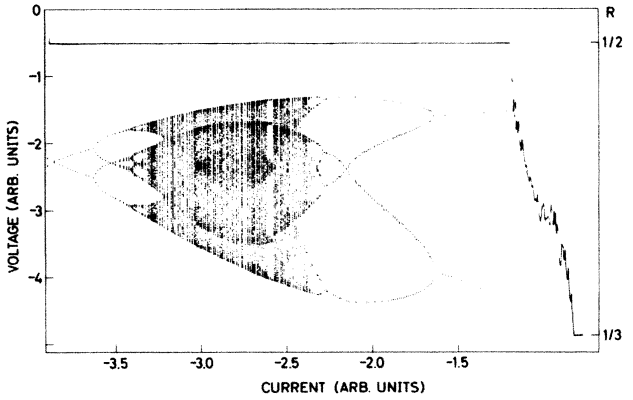

FIG. 14. Behavior on the $\frac{1}{2}$ step far below the critical line. $G=0.80$, $U(\phi)=\sin\phi$, $A=1$, and $\omega=1.76$. The I-R curve with the $\frac{1}{2}$ step is shown together with the Poincaré map of $\dot{\phi}$ as a function of the current. The ordinate to the left refers to the Poincaré map (arbitrary units), while the ordinate to the right refers to the I-R curve and displays the rotation number. A Feigenbaum bifurcation sequence into chaos and out again is clearly visible.

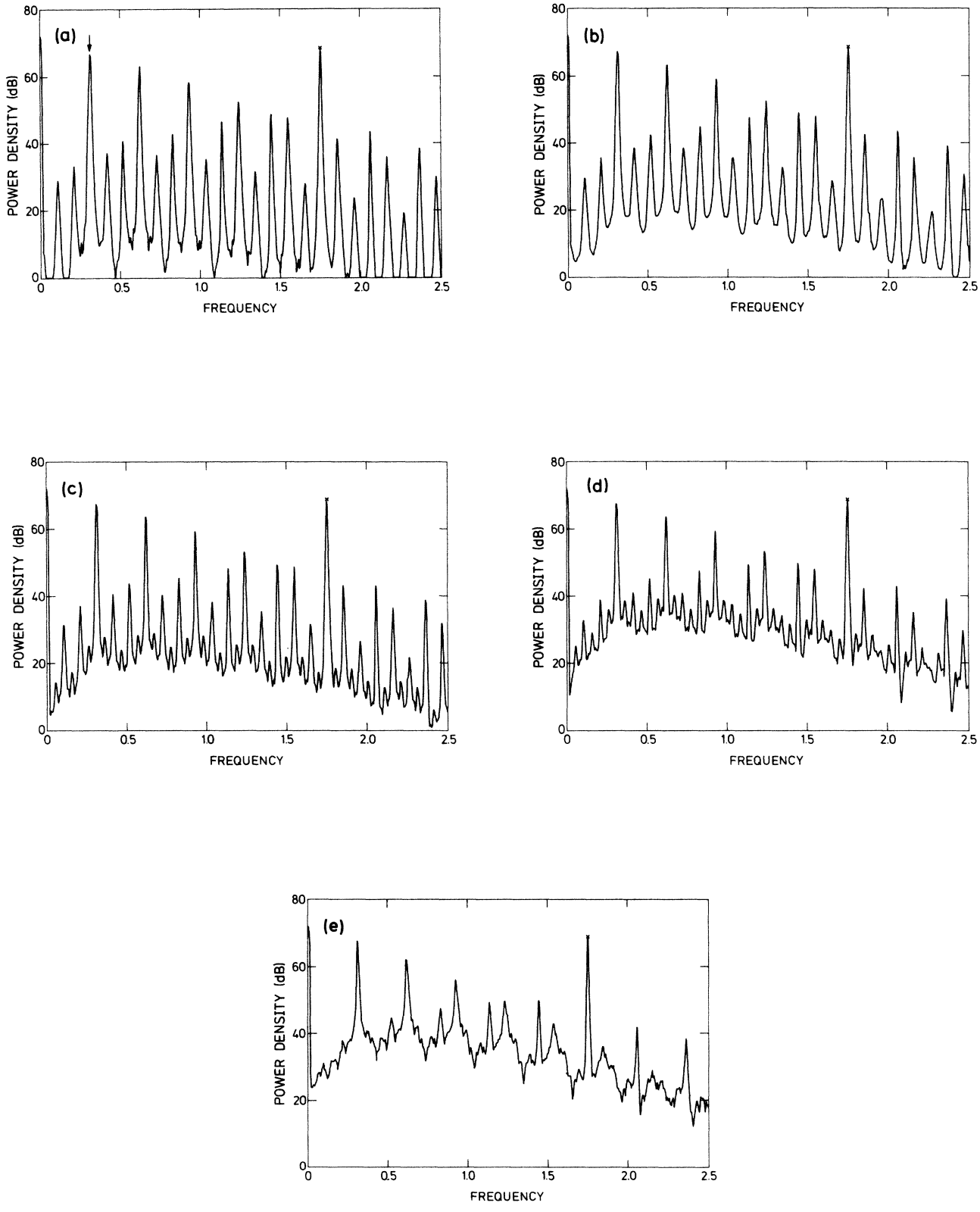

FIG. 15. Frequency spectra obtained at the rational rotation number $P/Q = \frac{3}{17}$. The external signal frequency ω is marked by a cross and the fundamental frequency $\langle \dot{\phi} \rangle$ by an arrow. The zero point on the ordinate is chosen arbitrarily. (a) is above the critical line, (b) on the critical line. In (c) and (d), period doubling is seen, and in (d) chaotic noise is present. In (e), phase lock is lost, as can be seen from the noise increase at low frequencies, and the background noise is highly chaotic.

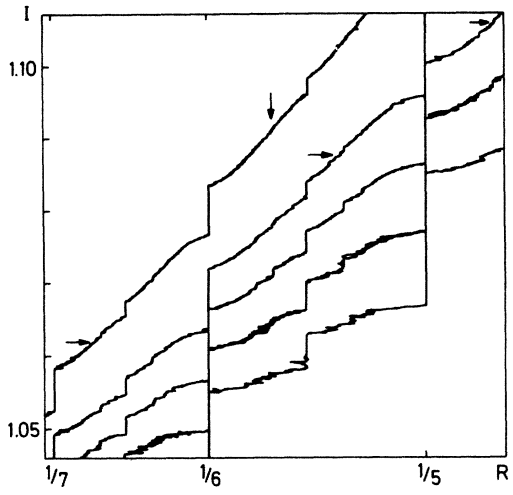

FIG. 16. Portions of I-R curves traversed by the critical line marked by horizontal arrows. $U(\phi)=\sin\phi$, $A=1$, $\omega=1.76$, and the G values are, from left to right, 1.51, 1.43, 1.39, 1.35, and 1.31. Associated frequency spectra taken at the rotation number $R=\frac{3}{17}$, marked by a vertical arrow, are shown in Fig. 15.

ground starts to increase. From the general behavior known for maps of the torus onto itself,[19] it seems to be a fair guess that this increase that is observed even before the bifurcation sequence sets in signals the onset of chaotic noise in the transient behavior, a phenomenon that might be connected with the observed excess noise in at least some of the parametric-amplifier configurations based on Josephson junctions.

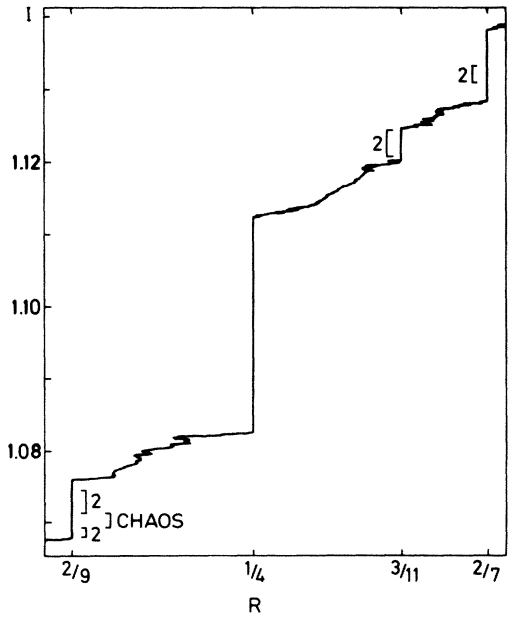

FIG. 17. Portion of an I-R curve lying slightly below the critical point. Intervals of bifurcations and chaos are indicated on the steps. $G=1.36$, $U(\phi)=\sin\phi$, $A=1$, and $\omega=1.76$.

TABLE II. Distances $|\varepsilon|$ (for the sine map) and ΔI (for the driven damped pendulum) for which the first bifurcation just occurs, and for which the chaotic regime is entered.

	$\lvert\varepsilon\rvert$		I_0-I	
P/Q	Bifurcation	Chaos	Bifurcation	Chaos
$\frac{1}{2}$	$\sqrt{2}-1$	0.89	0.17	0.27
$\frac{1}{3}$	0.26	0.48	0.05	0.11
$\frac{1}{4}$	0.19	0.30	0.03	0.06
$\frac{1}{5}$	0.15	0.25	0.02	0.05

For the large $1/Q$ step, we have in Table II listed the values of $|\varepsilon|$ [from (22)] and I_0-I, where the first bifurcation occurs, and where chaos is encountered. Typically, the values are smaller for smaller steps, see, e.g., the I-R curve in Fig. 17, which lies completely below the critical line. R is about 0.25 and all small steps are smeared out or have vanished into a seemingly disordered motion. While the $\frac{2}{7}$ as well as the $\frac{3}{11}$ step have bifurcated and chaos exists on the $\frac{2}{9}$ step, no bifurcations at all have yet occurred on the $\frac{1}{4}$ step. Additionally, we notice from the values in Table II that I_0-I decreases faster than $|\varepsilon|$ as Q is increased, in accordance with Eq. (60).

CONCLUSIONS

The universal scaling laws obtained by iterating circle maps of third order[3,6] have previously been shown to give a good description of the phase-locking structure along the critical line in systems with two competing frequencies such as the driven damped pendulum.[10] Above the critical line, the return map of the phase of the pendulum is one dimensional,[6] and therefore it is expected that the scaling as the critical line is approached can be discussed on the basis of the sine map. In particular, we have here investigated the scaling of the step sizes and the minimal distances, both regarding continued-fraction sequences and the average behavior. The former has been studied in the context of the convergence rate. As expected from renormalization analysis,[5] it is found that equivalence is a sufficient condition for numbers to exhibit the same scaling exponents. But, as shown, it is not a necessary condition. Nonequivalent numbers may have identical convergence rates, in which case a common scaling equation is produced. However, a condition of equal convergence rates is only a necessary condition and not sufficient for getting identical scaling exponents. Close to the crossover to chaos, scaling functions are found, and regarding the average behavior, these give rise to a definition of average measure and average correlation length exponents, which are related analogously to the more rigoristic defined quantities.

The self-similar step structure obtained along the critical line gives occasion for speculations on similarities with Cantor's discontinuum. To this end, two pseudodimensions have been defined; one, D_s, which is locally defined by using three steps only, corresponding to three successive rationals in a continued-fraction sequence, and anoth-

er, D_2, defined from the steps corresponding to rationals with a denominator of a power of 2. The former, subtracted from 1 is found to decay exponentially in the same way as the step sizes as the critical line is approached; the latter is found to lead to a decay of the step sizes in accordance with the decay obtained for Cantor's discontinuum, i.e., $D_2=D/2$.

The similarity dimension D_s is of special interest for the interpretation of experimental results since it offers a short-cut for determination of the fractal dimension in drastically reducing the amount of data needed. However, the observation that $1-D_s$ scales exponentially with the distance from the critical line raises severe doubt as to the reliability of the method.

In connection with this the rather surprising result of an analog-computer-based measurement of the decay exponent z for the driven damped pendulum is of particular interest. In contrast to other quantities, which agree closely with their sine-map counterparts, a large discrepancy (50% increase) is found for z. The most probable cause for this discrepancy is noise and an investigation of the influence of noise on the scaling behavior close to the critical line would therefore be of interest.

Below the critical line, the return map of the phase of the pendulum loses its one-dimensionality.[6,19] However, the one-dimensional sine map can still, at least qualitatively, be used to explain the behavior on the phase-locked steps as they pass the critical line into the chaotic regime. The larger steps (low Q values) keep growing until deep inside before bifurcation cascades into chaos develop. The smaller steps succumb to this close to the critical line. The utter chaos that develops is therefore partly caused by the overlapping of steps, partly due to the phase-locked steps breaking down from the inside through bifurcation sequences into chaos.

ACKNOWLEDGMENTS

We are indebted to T. Bohr, P. Grassberger, and M. H. Jensen for valuable and informative discussions. This work has been supported by the Danish Natural Science Research Council.

APPENDIX

In continuation of our numerical results we here show that renormalization-group analysis of circle homeomorphisms leads to the fact that periodic irrationals with convergence rates, which are identical, can be characterized by a common scaling equation.

Let $R=[a_1,\ldots,a_j,c_1,\ldots,c_k,c_1,\ldots,c_k,\ldots]$ be a continued fraction with period k, and $R_n=P_n/Q_n$ be the rationals defined as in (3). Then for $m\geqq 1$.

$$Q_{j+mk}=c_kQ_{j+mk-1}+Q_{j+mk-2}\,, \tag{A1}$$

and the same equality is valid for the P's. In matrix notation (A1) yields

$$\begin{bmatrix} Q_{j+mk} \\ Q_{j+mk-1} \end{bmatrix} = \begin{bmatrix} c_k & 1 \\ 1 & 0 \end{bmatrix} \begin{bmatrix} Q_{j+mk-1} \\ Q_{j+mk-2} \end{bmatrix}; \tag{A2}$$

thus

$$\begin{bmatrix} Q_{j+mk} \\ Q_{j+mk-1} \end{bmatrix} = \underline{C} \begin{bmatrix} Q_{j+(m-1)k} \\ Q_{j+(m-1)k-1} \end{bmatrix}, \tag{A3a}$$

where

$$\underline{C}= \begin{bmatrix} c_k & 1 \\ 1 & 0 \end{bmatrix} \begin{bmatrix} c_{k-1} & 1 \\ 1 & 0 \end{bmatrix} \cdots \begin{bmatrix} c_1 & 1 \\ 1 & 0 \end{bmatrix}. \tag{A3b}$$

Dividing by Q_{j+mk},

$$\begin{bmatrix} 1 \\ Q_{j+mk-1}/Q_{j+mk} \end{bmatrix} = \underline{C} \begin{bmatrix} 1 \\ Q_{j+(m-1)k-1}/Q_{j+(m-1)k} \end{bmatrix} \frac{Q_{j+(m-1)k}}{Q_{j+mk}}\,, \tag{A4}$$

we get from (16) in the limit $m\to\infty$,

$$\begin{bmatrix} 1 \\ \tilde{l} \end{bmatrix} = \underline{C} \begin{bmatrix} 1 \\ \tilde{l} \end{bmatrix} l^k\,, \tag{A5a}$$

where [cf. (15)]

$$\tilde{l}=[c_k,\ldots,c_1,c_k,\ldots,c_1,\ldots]\,, \tag{A5b}$$

and l is the convergence rate. Thus l is a root in the polynomial

$$P(r)=\det(\underline{C}r^k-\underline{E})\,. \tag{A6}$$

Here det denotes the determinant, and $\underline{E}$ is the unit matrix. (A6) can also be written

$$P(r)=Dr^{2k}-\mathrm{Tr}^k+1\,, \tag{A7}$$

where $D=\det(\underline{C})=(-1)^k$, and T is the trace of $\underline{C}$. The second root of $P(r)$ is seen to be $\beta=-1/l<-1$.

Now let f be some smooth (orientation-preserving) circle map, like the sine map defined by (19) and (22), with rotation number R. As usual,[4] $f^{(n)}$ and $f_{(n)}$ are defined from f,

$$f^{(n)}(r)=f^{Q_n}(r)-P_n \tag{A8}$$

and

$$f_{(n)}(r)=\alpha^n f^{(n)}(\alpha^{-n}r)\,, \tag{A9a}$$

where

$$\alpha=-l^{-x}\,. \tag{A9b}$$

Below, we will omit the variable r, e.g., we just write $f_{(n)}$ as $\alpha^n f^{(n)}\alpha^{-n}$. Let further $(M_m,\oplus)$ denote the group, generated by the elements $\binom{f}{g}$, where f and g are of the form $\alpha^{-i}f_{(j+mk+i)}\alpha^i$, and the addition

$$\begin{bmatrix} f_1 \\ g_1 \end{bmatrix} \oplus \begin{bmatrix} f_2 \\ g_2 \end{bmatrix} = \begin{bmatrix} f_1\circ f_2 \\ g_1\circ g_2 \end{bmatrix}, \tag{A10}$$

where $f\circ g$ denotes the composed function $f\circ g(r)=f(g(r))$. Note from the definition (A9) that $(M_m,\oplus)$ is commutative. In addition,

$$\alpha^{-ik}\begin{bmatrix} f \\ g \end{bmatrix}\alpha^{ik} = \begin{bmatrix} \alpha^{-ik}f\alpha^{ik} \\ \alpha^{-ik}g\alpha^{ik} \end{bmatrix} \tag{A11}$$

maps $\binom{f}{g}$ in M_{m+i} into an element in M_m. Since the set $\Lambda=\mathrm{GL}(2\mathbb{Z})$ of 2×2 integral matrices is an associative ring, we make $(M_m,\oplus)$ to a left Λ-module by defining a multiplication $\otimes$: $\Lambda\times M_m\to M_m$,

$$\begin{bmatrix} a & b \\ c & d \end{bmatrix}\otimes\begin{bmatrix} f \\ g \end{bmatrix}=\begin{bmatrix} f^a \\ f^c \end{bmatrix}\otimes\begin{bmatrix} g^b \\ g^d \end{bmatrix}, \tag{A12}$$

where, e.g., f^a means f composed a times. Analogous to (A3), we see that

$$\alpha^{-k}\begin{bmatrix} f_{(j+(m+1)k)} \\ \alpha f_{(j+(m+1)k-1)}\alpha^{-1} \end{bmatrix}\alpha^k=\underline{C}\otimes\begin{bmatrix} f_{(j+mk)} \\ \alpha f_{(j+mk-1)}\alpha^{-1} \end{bmatrix}. \tag{A13}$$

If R' is another periodic irrational with period k', and convergence rate $l'=l$, we have some matrix $\underline{C}'$ such that

$$(\alpha')^{-k'}\begin{bmatrix} f'_{(j'+(m+1)k')} \\ \alpha' f'_{(j'+(m+1)k'-1)}(\alpha')^{-1} \end{bmatrix}(\alpha')^{k'} =\underline{C}'\otimes\begin{bmatrix} f'_{(j'+mk')} \\ \alpha' f'_{(j'+mk'-1)}(\alpha')^{-1} \end{bmatrix}, \tag{A14}$$

where α', $f'_{(n)}$, j', and M'_m are defined analogous to α, $f_{(n)}$, j, and M_m. Furthermore, l is a root in the polynomial

$$P'(r)=\det(\underline{C}'r^{k'}-\underline{E}). \tag{A15}$$

If we for a moment regard Λ as embedded in the ring $\mathrm{GL}(2,\mathbb{R})$ of all 2×2 real matrices, matrices $\underline{S}$ and $\underline{S}'$ exist in $\mathrm{GL}(2,\mathbb{R})$ such that

$$\underline{C}=\underline{S}^{-1}\begin{bmatrix} \lambda_1 & 0 \\ 0 & \lambda_2 \end{bmatrix}\underline{S} \tag{A16a}$$

and

$$\underline{C}'=(\underline{S}')^{-1}\begin{bmatrix} \lambda'_1 & 0 \\ 0 & \lambda'_2 \end{bmatrix}\underline{S}', \tag{A16b}$$

where

$$\lambda_1=(-l)^k,\quad \lambda_2=l^{-k},\qquad \lambda'_1=(-l)^{k'},\quad \lambda'_2=l^{-k'}. \tag{A16c}$$

Hence,

$$(\underline{C}')^k=(\underline{S}')^{-1}\underline{S}\,\underline{C}^{k'}\underline{S}^{-1}\underline{S}' =(\underline{S}^{-1}\underline{S}')^{-1}\underline{C}^{k'}(\underline{S}^{-1}\underline{S}')=\underline{\tilde{S}}^{-1}\underline{C}^{k'}\underline{\tilde{S}}, \tag{A17a}$$

with

$$\underline{\tilde{S}}=\underline{S}^{-1}\underline{S}'. \tag{A17b}$$

Noting that $\underline{C}^{k'}$ and $(\underline{C}')^k$ therefore have the same determinant and trace, $\underline{\tilde{S}}$ can be chosen in Λ, e.g., if

$$\underline{C}^{k'}=\begin{bmatrix} c_1 & c_2 \\ c_3 & c_4 \end{bmatrix},$$

and

$$(\underline{C}')^k=\begin{bmatrix} c'_1 & c'_2 \\ c'_3 & c'_4 \end{bmatrix}, \tag{A18}$$

take

$$\underline{\tilde{S}}=\begin{bmatrix} c_1-c'_4 & c'_2 \\ c_3 & 0 \end{bmatrix}.$$

We notice that since $c_1\geqq c_4$, and $c'_1\geqq c'_4$, then $c_1-c'_4=c'_1-c_4=\frac{1}{2}(c_1+c_4)+\frac{1}{2}(c'_1+c'_4)-(c_4+c'_4)\geqq 0$.

Finally, we get

$$\alpha^{-kk'}\begin{bmatrix} f_{(j+(m+k')k)} \\ \alpha f_{(j+(m+k')k-1)}\alpha^{-1} \end{bmatrix}\alpha^{kk'} =\underline{C}^{k'}\otimes\begin{bmatrix} f_{(j+mk)} \\ \alpha f_{(j+mk-1)}\alpha^{-1} \end{bmatrix}, \tag{A19}$$

while

$$(\alpha')^{-kk'}\begin{bmatrix} f'_{(j'+(m+k)k')} \\ \alpha' f'_{(j'+(m+k)k'-1)}(\alpha')^{-1} \end{bmatrix}(\alpha')^{kk'} =(\underline{C}')^k\otimes\begin{bmatrix} f'_{(j'+mk')} \\ \alpha' f'_{(j'+mk'-1)}(\alpha')^{-1} \end{bmatrix} \tag{A20a}$$

by (A17) gives

$$(\alpha')^{-kk'}\left[\underline{\tilde{S}}\otimes\begin{bmatrix} f'_{(j'+(m+k)k')} \\ \alpha' f'_{(j'+(m+k)k'-1)}(\alpha')^{-1} \end{bmatrix}\right](\alpha')^{kk'} =\underline{C}^{k'}\otimes\left[\underline{\tilde{S}}\otimes\begin{bmatrix} f'_{(j'+mk')} \\ \alpha' f'_{(j'+mk'-1)}(\alpha')^{-1} \end{bmatrix}\right]. \tag{A20b}$$

Above, it is used that generally for $\underline{A}$ in Λ and $\binom{f}{g}$ in M_{m+i}, one has in M_m

$$\underline{A}\otimes\left[\alpha^{-ik}\begin{bmatrix} f \\ g \end{bmatrix}\alpha^{ik}\right]=\alpha^{-ik}\left[\underline{A}\otimes\begin{bmatrix} f \\ g \end{bmatrix}\right]\alpha^{ik}. \tag{A21}$$

Equation (A19) and (A20) show that renormalization-group analysis leads to the same equation in the limit $m\to\infty$. Since only a finite number of periodic irrationals with convergence rate equal to l exist, the procedure above can be used successively taking one more number into account each time. Hence, we end up with a common scaling equation, and the proof is done. Conversely, it is seen that periodic irrationals with different convergence rates cannot be associated with a common scaling equation.

*Present address: Nordisk Institut for Teoretisk Atomfysik (NORDITA), Blegdamsvej 17, DK-2100 Copenhagen Ø, Denmark.

[1]M. J. Feigenbaum, J. Stat. Phys. **19**, 25 (1978); **21**, 669 (1979).

[2]P. Grassberger, J. Stat. Phys. **26**, 173 (1981); P. Grassberger and I. Procaccia, Phys. Rev. Lett. **50**, 346 (1983).

[3]S. J. Shenker, Physica (Utrecht) **5D**, 405 (1982).

[4]M. J. Feigenbaum, L. P. Kadanoff, and S. J. Shenker, Physica (Utrecht) **5D**, 370 (1982).

[5]D. Rand, S. Ostlund, J. Sethna, and E. Siggia, Phys. Rev. Lett. **49**, 132 (1982); Physica (Utrecht) **8D**, 303 (1983).

[6]P. Bak, T. Bohr, M. H. Jensen, and P. V. Christiansen, Solid State Commun. **51**, 231 (1984); M. H. Jensen, P. Bak, and T. Bohr, Phys. Rev. Lett. **50**, 1637 (1983); Phys. Rev. A **30**, 1960 (1984); **30**, 1970 (1984).

[7]P. Cvitanović, M. H. Jensen, L. P. Kadanoff, and I. Procaccia, Phys. Rev. Lett. **55**, 343 (1985).

[8]L. Glass and R. Perez, Phys. Rev. Lett. **48**, 1772 (1982); Phys. Lett. **90A**, 441 (1982); L. Glass and M. R. Guevara, J. Math. Biol. **14**, 1 (1982); L. Glass, M. R. Guevara, and A. Shrier, Physica (Utrecht) **7D**, 89 (1983).

[9]M. T. Levinsen, J. Appl. Phys. **53**, 4294 (1982).

[10]P. Alstrøm, M. H. Jensen, and M. T. Levinsen, Phys. Lett. **103A**, 171 (1984); P. Alstrøm and M. T. Levinsen, Phys. Rev. B **31**, 2753 (1985); **32**, 1503 (1985).

[11]W. J. Yeh, Da-Ren He, and Y. H. Kao, Phys. Rev. Lett. **52**, 480 (1984); Phys. Rev. B **30**, 172 (1984).

[12]G. Cantor, Math. Ann. **21**, 545 (1883).

[13]B. B. Mandelbrot, *The Fractal Geometry of Nature* (Freeman, San Francisco, 1982).

[14]See, e.g., *Elementary Stability and Bifurcation Theory*, edited by G. Iooss and D. D. Joseph (Springer-Verlag, New York, 1980), p.223.

[15]See, e.g., L. K. Hua, *Introduction to Number Theory* (Springer-Verlag, Berlin, 1982), pp. 258 and 259.

[16]A. Denjoy, J. Math. Pures Appl. **11**, 333 (1932).

[17]F. Hausdorff, Math. Ann. **79**, 157 (1919).

[18]T. C. Halsey, M. H. Jensen, L.P. Kadanoff, I. Procaccia, and B. I. Shraiman, Phys. Rev. A **33**, 1141 (1986), **34**, 1601(E) (1986); M. H. Jensen, L. P. Kadanoff, A. Libchaber, I. Procaccia, and J. Stavans, Phys. Rev. Lett. **55**, 2798 (1985); M. H. Jensen (private communication).

[19]T. Bohr, Phys. Rev. Lett. **54**, 1737 (1985).